Feasibility of using alternative swabs and storage solutions for paired SARS-CoV-2 detection and microbiome analysis in the hospital environment

Running Title: Alternative swabs for COVID-19 screening and microbiome analysis

Jeremiah J. Minich[1], Farhana Ali[2], Clarisse Marotz[3], Pedro Belda-Ferre[3], Leslie Chiang[4], Justin P. Shaffer[3], Carolina S. Carpenter[5], Daniel McDonald[3], Jack Gilbert1[1,3,5], Sarah M. Allard[3], Eric E Allen[1,5,6], Rob Knight[3,5,7,8], Daniel A. Sweeney[9], Austin D. Swafford[5#]

1. Marine Biology Research Division, Scripps Institution of Oceanography, University of California San Diego, La Jolla, CA, USA.
2. Division of Gastroenterology, Department of Pediatrics, University of California San Diego, La Jolla, CA, USA.
3. Department of Pediatrics, School of Medicine, University of California San Diego, La Jolla, CA, USA.
4. Division of Infectious Diseases, Department of Pediatrics, University of California San Diego, La Jolla, CA, USA.
5. Center for Microbiome Innovation, University of California San Diego, La Jolla, CA, USA.
6. Division of Biological Sciences, University of California San Diego, La Jolla, CA, USA.
7. Department of Computer Science and Engineering, University of California San Diego, La Jolla, CA, USA.
8. Department of Bioengineering, University of California San Diego, La Jolla, CA, USA.
9. Division of Pulmonary, Critical Care, and Sleep Medicine, Department of Internal Medicine, University of California, San Diego, La Jolla, CA, USA.

#Corresponding author: adswafford@ucsd.edu and dasweeney@health.ucsd.edu

30 **Abstract**

31 **Background**

32 Determining the role of fomites in the transmission of SARS-CoV-2 is essential in the hospital setting and
33 will likely be important outside of medical facilities as governments around the world make plans to ease
34 COVID-19 public health restrictions and attempt to safely reopen economies. Expanding COVID-19
35 testing to include environmental surfaces would ideally be performed with inexpensive swabs that could
36 be transported safely without concern of being a source of new infections. However, CDC-approved
37 clinical-grade sampling supplies and techniques using a polyester swab are expensive, potentially expose
38 laboratory workers to viable virus and prohibit analysis of the microbiome due to the presence of
39 antibiotics in viral transport media (VTM). To this end, we performed a series of experiments comparing
40 the diagnostic yield using five consumer-grade swabs (including plastic and wood shafts and various head
41 materials including cotton, polyester, and foam) and one clinical grade swab for inhibition to RNA. For
42 three of these swabs, we evaluated performance to detect SARS-CoV-2 in twenty intensive care unit
43 (ICU) hospital rooms of patients with 16 COVID-19+. All swabs were placed in 95% ethanol and further
44 evaluated in terms of RNase activity. SARS-CoV-2 was measured both directly from the swab and from
45 the swab eluent.

46 **Results**

47 Compared to samples collected in VTM, 95% ethanol demonstrated significant inhibition properties
48 against RNases. When extracting directly from the swab head as opposed to the eluent, RNA recovery
49 was approximately 2-4x higher from all six swab types tested as compared to the clinical standard of
50 testing the eluent from a CDC-approved polyester swab. The limit of detection (LoD) of SARs-CoV-2
51 from floor samples collected using the CGp or TMI swabs was similar or better than the CDC standard,
52 further suggesting that swab type does not impact RNA recovery as measured by SARs-CoV-2. The LoD
53 for TMI was between 0-362.5 viral particles while PE and CGp were both between 725-1450 particles.
54 Lastly microbiome analyses (16S rRNA) of paired samples (e.g., environment to host) collected using
55 different swab types in triplicate indicated that microbial communities were not impacted by swab type

but instead driven by the patient and sample type (floor or nasal).

Conclusions

Compared to using a clinical-grade polyester swab, detection of SARS-CoV-2 from environmental samples collected from ICU rooms of patients with COVID was similar using consumer grade swabs, stored in 95% ethanol. The yield was best from the swab head rather than the eluent and the low level of RNase activity in these samples makes it possible to perform concomitant microbiome analysis.

Keywords:

COVID-19, SARS-CoV-2, RT-qPCR, swab, global health

Background

Since its appearance in early December of 2019, Severe acute respiratory syndrome coronavirus 2 (SARS-CoV-2), the causative agent of coronavirus disease 2019 (COVID-19), has spread to 197 countries resulting in a total of 539,906 deaths and 11,669,259 confirmed cases as of July 8, 2020[1]. As health officials rush to contain the spread of the disease, federal governments are combating the economic fallout, and there is a pressing need to reopen the economies albeit safely, gradually, and in stages. Large-scale testing and contact tracing remain key for controlling viral spread. In addition,; environmental sampling of microbes can support the epidemiologic investigations of disease outbreaks [2,3] and shows promise for monitoring SARS-CoV-2. However, there are supply and cost limitations with the products currently recommended required by the CDC protocol for sample collection supplies. For example, personal protective equipment, swabs and, viral transport medium (VTM), and personal protective equipment (PPE) are being depleted in developed nations like the United States, and are in even shorter supply in resource limited settings including low- and middle-income countries (3). Broad SARS-CoV-2 surveillance requires microbiologic surface fomite sampling protocols, the efficacy of which hinges on requires inexpensive, readily available swabs and collection reagents to support the large

82 sample sizes at geographic scales necessary to inform public health policy., and the growing need for
83 environmental testing will place additional demands on current swab supplies.
84
85 The use of the U.S. Centers for Disease Control (CDC)-recommended viral transport media (VTM) places
86 an additional barrier to efficient and safe deployment of screening and sampling measures. VTM
87 maintains viral viability and therefore the CDC recommends that all samples be handled in a biosafety
88 level-2 (BSL-2) laboratory . VTM also contains antimicrobial agents that limit the type of research
89 studies into likely to interfere with downstream assessment of the microbial context of SARS-CoV-2,
90 such as microbial relationships with that may enable new insights into viral susceptibility and resistance
91 as demonstrated by several recent reports [4–6]. Using inactivating sample collection solutions, such as
92 microbiome assay-compatible alcohols, would increase the number of testing laboratories capable of
93 performing SARS-CoV-2 screening, and ameliorate the risks associated with sample transport and
94 processing. Given these considerations, validation of alternative strategies such as self-administered
95 testing using consumer-grade materials and inactivating storage media is urgently needed.
96 There are aspects of both the swab and the transport media which must be considered when developing a
97 testing procedure for SARS-CoV-2. From a microbiome perspective, the primary concern with using
98 alternative media and consumer-grade materials is the risk of contaminant RNases and/or PCR inhibitors.
99 The presence of these molecules would increase the false negative rate of SARS-CoV-2 RNA by either
100 degrading the virus, or interfering with reverse transcription and quantitative polymerase chain reactions
101 (RT-qPCR) which are the basis for SARS-CoV-2 testing [7]. In addition, the ability to extract the virus
102 from either the swab or the swab eluent must be elucidated. The fixative property of ethanol could result
103 in nucleic acids adhering to swab heads, reducing the ability to measure SARS-CoV-2 RNA from the
104 swab eluent [6]. To fully address these concerns, large screening efforts comparing the recommended and
105 alternative collection methods are needed. However, given the present scale and urgency of the COVID-
106 19 pandemic outbreak, limiting this comparison to a small number of viable options would greatly
107 expedite providing guidance for alternatives to the supply chain this process while minimizing costs. Here

108 we characterize the suitability of detecting SARS-CoV-2 RNA in experimental conditions as well as
109 COVID-19 patient and built-environment samples using viral-inactivating storage solutions and
110 alternative medical-grade and consumer-grade swabs.
111
112 **Materials and Methods**

113 *VTM versus EtOH sample comparison*

114 Nasopharyngeal (NP) swabs were collected from COVID-19 positive individuals (n=39) according to CDC
115 guidelines and were stored in viral transport media (VTM) and transported to the lab on dry ice. For
116 comparison, sterile polyester-head, plastic-shaft ('PE', BBL Culture swab REF-220135, Becton, Dickinson
117 and Company) were used to collect nares samples by rotating the dry swab head in the nares for
118 approximately 10 seconds from lab members, COVID-19 patients (n=11), or healthcare workers (n=11) in
119 the Hillcrest ICU, and then immediately placed in 95% ethanol (EtOH), and transported to the lab on dry
120 ice. Eluent nucleic acid extractions were performed on 200 µL of the swab eluent (either VTM or EtOH)
121 using the Omega Mag-Bind® Viral DNA/RNA 96 Kit (catalog# M6246-03), which only uses chemical
122 lysis and does not include a bead beating step. For nucleic acid extraction from the swab head, the MagMAX
123 Microbiome Ultra kit (Cat#A42357, Thermo Fisher Scientific) was used. For the direct comparison of
124 SARS-CoV-2 extraction efficiency, we extracted EtOH eluent and swab separately from the same samples
125 of COVID-19 patients (n=24) with approval of the UC San Diego Institutional Review Board under
126 protocols #150275 and #200613.
127
128 *RT-qPCR for VTM and 95% EtOH comparison using polyester-tipped plastic swabs*

129 SARS-CoV-2 detection was performed following a miniaturized version of the CDC protocol. Each RT-
130 qPCR reaction contained 4 µL RNA template, 100 nM forward and reverse primers, 200 nM probe, 3 µl
131 TaqPath (catalog# A15299, Thermo), and RNase-free water to a total reaction volume of 10 µl. All primers
132 and probes were ordered from IDT (catalog# 10006606). RT-qPCR was performed on the Bio-Rad CFX384
133 Touch Real-Time PCR Detection System following the CDC thermocycling guidelines. Serial dilutions of
134 the Hs_RPP30 Positive Control plasmid (catalog# 10006626, IDT) or 2019-nCoV_N_Positive Control

135 plasmid (catalog# 10006625, IDT) were included to extrapolate human RNase P (Rp) and SARS-CoV-2
136 copy numbers, respectively. The SARS-CoV-2 N1 marker gene was used for detection and quantitation
137 [8][9].
138
139 *Validation of use of alternative swabs (testing inhibition of SARS-CoV-2 detection)*
140 The standard swab type approved for use in SARS-CoV-2 detection is a synthetic fiber swab with a plastic
141 or wire shaft polyester head. In addition to a CDC approved device, we tested an additional five alternative
142 swabs that included both plastic and wood materials for the shaft and polyester, foam, or cotton materials
143 for the swab head. The exact devices used were sterile rayon polyester-head, plastic-shaft ('PE', BBL
144 Culture swab REF-220135, Becton, Dickinson and Company); sterile foam-head, plastic-shaft ('BDF',
145 Flock PurFlock REF-25-3606-U-BT, Becton, Dickinson and Company); non-sterile cotton-head, plastic-
146 shaft in use by The Microsetta Initiative ('TMI', SKU#839-PPCS, Puritan Medical Products); non-sterile
147 cotton-head plastic-shaft consumer-grade ('CGp' Part #165902, CVS Caremark Corp.); non-sterile cotton-
148 head wooden-shaft consumer-grade ('CGw', Part#858948, CVS Caremark Corp.); and non-sterile cotton-
149 head, wooden-shaft ('Pu', REF-806-WC, Puritan Medical Products). The goal was to evaluate if detection
150 of SARS-CoV-2 was reduced with certain swab types from both the eluent (standard protocol) and swab
151 head directly (new method). A total of six swab types were compared and All swabs were processed
152 following the standard SARS-CoV-2 protocol provided by the CDC [6]. The six swab types were used:
153 sterile rayon polyester-head, plastic-shaft ('PE', BBL Culture swab REF-220135, Becton, Dickinson and
154 Company); sterile foam-head, plastic-shaft ('BDF', Flock PurFlock REF-25-3606-U-BT, Becton,
155 Dickinson and Company); non-sterile cotton-head, plastic-shaft in use by The Microsetta Initiative ('TMI',
156 SKU#839-PPCS, Puritan Medical Products); non-sterile cotton-head plastic-shaft consumer-grade ('CGp'
157 Part #165902, CVS Caremark Corp.); non-sterile cotton-head wooden-shaft consumer-grade ('CGw',
158 Part#858948, CVS Caremark Corp.); and non-sterile cotton-head, wooden-shaft ('Pu', REF-806-WC,
159 Puritan Medical Products). To evaluate if the raw swab materials had any background contaminants such
160 as RNase, which would decrease the sensitivity, we added 600 ng of purified, DNA-free human lung RNA

161 (Cat#AM7968, Thermo Fisher Scientific) onto each of the six swab types in triplicate and immediately
162 stored in two storage solutions (500 µL 95% EtOH and 500 µL 91% isopropanol). Separately, two sets of
163 six, 10-fold serial dilutions of human RNA were included as controls directly.
164
165 The same quantity of human RNA (600 ng) along with an equal volume (5 µL) of SARS-CoV-2 RNA was
166 added to either 95% EtOH (n=3) or 91% isopropanol (n=3) in the presence of 0, 2.5, and 25 µg RNaseA (in
167 triplicate) to assess any inhibition offered against RNase contaminants. Four negative (swab only) and four
168 positive (swab + 600 ng spiked human RNA + 5 µL spiked SARS-CoV-2 RNA [~20,000 copies per µL])
169 controls were included.
170
171 *Limit of detection comparison of swabs using floor as substrate*
172 To estimate the limit of detection and compare the viral yield across three swab types (PE, CGp, and
173 TMI), a serial dilution of viral particles was spiked onto floor swabs. In brief, separate 25 cm x 25 cm
174 areas of the floor from a low-traffic common room inside a building with no SARS-CoV-2 research
175 activities (i.e., Marine Biology research building at UC San Diego) were swabbed with a total of 24 swabs
176 per swab type. Swabs were processed in groups of six by swabbing a quarter of that 625-cm^2 space, with
177 each swab ultimately covering an *ca.* 26-cm^2 area, the similar surface area (25 cm^2) used for detection of
178 low biomass samples in JPL spacecraft assembly clean rooms based on previous work in the JPL
179 spacecraft assembly facility [10]. Swabs were then stored at room temperature for *ca.* 1 hr in a 2-mL
180 deep-well 96-well plate during transport back to a BSL-2 laboratory at UC San Diego. A single serial
181 dilution of SARS-CoV-2 viral particles [BEI Resources: Cat# 52286, Lot# 70033548] was made at the
182 following concentrations: 232000, 2320, 1160, 580, 290, 145, and 72.5 viral particles per µL. A total of 5
183 µL of each dilution, or water as a negative control, was pipetted onto each swab type in triplicate and then
184 immediately placed into 95% EtOH. Swabs in EtOH were then stored overnight at -80°C until processing.
185 Upon processing, an additional 24 'no swab' controls were included whereby 5 µL of the dilutions were
186 dispensed directly into the extraction plate lysis buffer. Samples were processed using the same nucleic
187 extraction method as described for swab heads above, and eluted in 75 µL of elution buffer. For RT-

188 qPCR, 5 µL of template was used for each marker N1 and Rp. To address potential issues of non-
189 normality, total copies were compared across swab types at each individual dilution using Kruskal-Wallis
190 tests with Benjamini-Hochberg FDR 0.05 post-hoc test.
191
192 *Patient and hospital environmental sampling*
193 All study patients were hospitalized with clinical concerns for COVID-19 and received standard diagnostic
194 testing. Study samples were collected from subjects' nares or hospital surfaces using three dry swab types
195 (PE, TMI, CGp) under the UC San Diego Institutional Review Board protocol #150275 and #200613. Both
196 nasal samples and hospital surfaces were collected using three dry swab types (PE, TMI, CGp). Nasal
197 samples were collected by inserting the swab into one nostril to the depth of approximately 2-3 cm and
198 rotated for 5-10 seconds. Hospital surfaces sampled included the floor inside the patient's room (*ca.* 625-
199 cm^2 area) and the patient's bedrail. All swabs were immediately placed in a collection tube containing 0.5-
200 1.0 mL 95% EtOH, stored on dry ice, and processed for RNA or total nucleic acid extraction
201 (Supplementary Methods).
202
203 *Extraction and RT-qPCR of hospital swabs and controls*
204 All swab comparison- and hospital samples were processed according to the manufacturer's protocol using
205 the MagMAX Microbiome Ultra kit (Cat#A42357, Thermo Fisher Scientific), and eluted into 70 µL buffer.
206 For RT-qPCR, 5 µL sample was processed using the standard SARS-CoV-2 protocol provided by the CDC
207 (Cat# 2019-nCoVEUA-01[11]).
208
209 *Microbiome processing and analysis*
210 A subset of 40 samples were processed for 16S rRNA sequencing using established EMP protocols
211 (https://earthmicrobiome.org/protocols-and-standards/16s/). These included 18 floor samples, 21 nasal
212 samples, and 1 negative control. Floor samples included all triplicates from the three swab types (PE, TMI,
213 and CGp) from two patient rooms (patient 7 and 18). The nasal samples included triplicates of all three
214 swab types from patient 1, triplicates of PE and CGp from patient 7, and triplicates of PE and TMI from

215 patient 18. The same previously extracted nucleic acid template, which was concurrently used for RT-
216 qPCR, was used as template for 16S rDNA library generation (amplifying the DNA). Specifically, 0.4 µL
217 of nucleic acid was processed in 10 µL 16S rRNA PCR reactions following the miniaturized protocol [12]
218 using the 515f/806r EMP primers, and sequenced on an Illumina MiSeq [13–16]. Samples were then
219 processed in Qiita (Study ID 13275) [17] and analyzed using the QIIME2 [18,19] [version?] pipeline with
220 Deblur [20] 1.1.0 as the method of sOTU generation. Samples were visualized in PCoA plots in Qiita using
221 EMPeror [21]. Beta diversity was calculated using Unweighted Unifrac and compared with PERMANOVA
222 (999 permutations).
223
224 *Statistics and visualizations*
225 Visualizations and statistical comparisons performed using PRISM 8.0 and the limit of detection
226 determination were consistent with CDC recommendations whereby samples with a Ct value greater than
227 40 were omitted [8].
228
229 **Results**
230 Our experimental design sought to answer three primary questions: whether the efficacy of SARS-CoV-2
231 detection is influenced by the following three variables: 1) does the swab storage solution (95% EtOH vs
232 91% isopropanol) impact the sensitivity of detection; 2) which sample fraction, swab head or eluent,
233 provides better detection fidelity; and 3) does the swab head material type matter? To do this we designed
234 a series of experiments to compare RNA recovery as measured by RT-qPCR using multiple swab types and
235 storage solutions. We additionally did environmental sampling in a hospital environment with a subset of
236 swab types for comparison.
237
238 *Feasibility of 95% EtOH for sample storage and extraction from use of swab head rather than eluent*
239 To evaluate the feasibility of switching from VTM to a more readily-available, viral-inactivating sample
240 collection solution, we compared the extraction efficiency of polyester-tipped plastic-shafted

241 nasopharyngeal (NP) swab samples stored in VTM versus nasal samples collected using CDC-
242 recommended polyester-tipped plastic-shafted (PE) swabs stored in 95% ethanol (EtOH). When mirroring
243 the CDC protocol, which calls for extraction from 200 µL of the eluent from VTM surrounding NP swabs,
244 we had significantly lower recovery of human RNA in 95% EtOH eluent compared to VTM (Figure 1a;
245 one-way ANOVA with Tukey's multiple comparison, VTM eluent vs. EtOH eluent $p<0.001$). However,
246 similar levels of human RNA were recovered when extracting from the EtOH-preserved swab head itself
247 (Figure 1a; one-way ANOVA with Tukey's multiple comparison, VTM vs. EtOH swab $p=0.3$). In a subset
248 of seven COVID-19 patient nares samples stored in 95% EtOH, we also detected significantly higher
249 SARS-CoV-2 viral load in RNA extracted from the swab head versus eluent (Figure 1b; one-tailed paired
250 Student's *t*-test $p=0.03$).
251
252 To more quantitatively determine the effects of alcohol-based preservation media, we extracted RNA from
253 a pure, commercial sample of human RNA added to water, EtOH, or 91% isopropanol, and found no impact
254 on extraction efficiency (Figure 1c; one-way ANOVA, $p>0.05$). Next, we examined whether alcohol
255 storage solutions had any protective properties of RNA, specifically a possible inhibitory effect on RNases
256 that might be present in the environment. If alcohol inhibits the RNaseA, one would expect to see similar
257 amounts of RNA as without RNaseA added in control experiments. In the presence of abundant RNaseA
258 added to the solution, 95% EtOH protected both human RNA and SARS-CoV-2 RNA better than 91%
259 isopropanol. Only a moderate decrease in total RNA recovery was observed, at the most extreme
260 concentration of 25 mg per reaction, which is equivalent to the standard amount used for RNA removal
261 during DNA extraction (Figure 1d).
262
263 *Comparison of alternative swab types against standard CDC approved polyester swab*
264 Given that the performance of eluent vs. swab-based extractions in each alcohol may depend on the swab
265 tip and body composition, we next tested RNA recovery from both the swab head and the surrounding
266 eluent from a range of medical- and consumer-grade swabs (Methods) (Figure 1e). The RNA yield was
267 highest from swab heads compared to eluent regardless of the swab type and whether stored in 95% EtOH

268 (p<0.0001, U=37, Mann-Whitney) or 91% isopropanol (P<0.0001, U=28, Mann-Whitney) (Figure 1e-f).
269 The storage solution did not impact RNA quality (Supplemental Figure 1b, Mann-Whitney, p>0.05),
270 although swab type had a minor impact (Supplemental Figure 1c, Kruskal-Wallis p=0.03, KW=12.17)[22].
271 To compare impacts of various alternative swabs, we normalized the recovery of each test to PE eluent,
272 indicated by '1' (Figure 1e), which is the standard CDC approved method. Thus, any sample with a value
273 greater than 1 would indicate an enhanced recovery of RNA, whereby less than 1 indicates a lower recovery
274 of RNA compared to the standard. The RNA recovery ratio of swab-to-eluent and total yield varied among
275 swab type (p<0.0001, KW=28.37, Kruskal-Wallis for eluent, and p<0.0001, KW=15.43, Kruskal-Wallis
276 for swab heads) (Supplemental Figure 2). This difference in performance may relate to the differences in
277 observed adsorption capacity across swab types (Shapiro-Wilkes p=0.1, w=0.8357; ANOVA p=0.0001,
278 F=7.5, R^2=0.56). TMI adsorbed the least (84.5 µL, 20.4; mean, SD) followed by plastic shafts (PE: 141 µL,
279 23.1; CGp: 143.3 µL, 29.9) (Supplemental Figure 3). CGp swabs had the highest recovery of RNA from
280 the swab head, while TMI swabs had the highest overall recovery of RNA when combining both eluent and
281 direct swab extractions (Figure 1e, Supplemental Figure 2).
282
283 *SARSs-CoV-2 limit of detection comparison across swab types*
284 We next assessed whether the swab type used would impact the recovery of SARS-CoV-2 and alter the
285 limit of detection when using non-CDC-recommended swabs (CGp or TMI compared to PE). All negative
286 controls for floor swabs were indeed negative for SARS-CoV-2 using N1 and N2 (Supplemental Table 1,
287 Figure 2) and all 'no-swab' controls which only had SARS-CoV-2, were negative for human Rp
288 (Supplemental Table 1). For the 'no-swab' and TMI swab, SARS-CoV-2 was detected in all of the three
289 replicates at the lowest input of 362.5 genome equivalents 'GE', whereas the lowest dilution for all three
290 replicates to be positive for CGp and PE swabs was 1450 GE (Supplemental Table 1, Figure 2a). This
291 suggests the limit of detection for neat and TMI swabs is likely between 0 and 362.5 GE per reaction
292 whereas both CGp and PE were less sensitive with an expected limit between 750 and 1450 GE per reaction.
293 There was a strong correlation between the input or theoretical GE and the measured GE with slopes all

294 greater than 0.95 and the R^2>0.96. Despite TMI appearing to have the best overall performance in SARSs-
295 CoV-2 detection followed by PE and then CGp, the total viral yield did not differ across swab types at the
296 lowest dilution of 362.5 (P>0.05, Kruskal-Wallis test) (Figure 2a). Specifically, multiple post-hoc
297 comparisons showed that variation across swab-type only existed at the highest concentration (116,000 GE)
298 with the TMI swabs having a higher viral recovery compared to PE swabs (P=0.04, KW=7.21) (Figure 2).
299 Rp yield was also compared across swab types and across viral inputs to characterize the variation in input
300 biomass. For each swab type, human Rp gene was equally detected across the titrations indicating the swab
301 method was sufficiently controlled (Supplemental Figure 4a). Swab type, however, did suggest that the Rp
302 gene was highest in the PE swab as compared to the CGp and TMI swabs (Kruskal-Wallis: P<0.0001,
303 KW=41.41) (Supplemental Figure 4b). This result suggests that PE swabs may adsorb more biomass.
304 However, when we compared the variation in Cq values of hospital samples of nares and floor from the
305 same hospital using PE swabs, we observed Rp values that varied over six orders of magnitude
306 (Supplemental Figure S5), much greater than the three orders of magnitude observed across swab types.
307 Specifically, for floor samples, the Rp yield (copies per extraction) range across swab types was 149-3368
308 copies for PE, 0-3980 for CGp, and 0-207 for TMI.
309
310 *Hospital proof of concept study*
311 Based on the results from these initial experiments, we conducted a proof-of-concept study in the clinical
312 setting by performing RT-qPCR for the SARS-CoV-2 N1 amplicon and human RNase P gene on RNA
313 extracted from the swab head of nasal samples collected using TMI and/or CGp swabs alongside the
314 recommended PE swabs. Of the 20 participants sampled, 16 tested positive for SARS-CoV-2 at admission
315 and were designated as COVID-19(+). The average time from diagnosis to sampling was *ca.* 4.2 days, with
316 a NP swab test occurring within 72 hours of the time of nasal sampling. Of the 12 nasal samples using the
317 PE swab preserved in EtOH from COVID-19(+) patients, nine were positive for the presence of SARS-
318 CoV-2 or a false negative rate of 25% (Figure 3a) compared to 14/16 SARS-CoV-2 positive NP swabs for
319 the same group of patients, a false negative rate of 12.5%. For CGp and TMI swabs, 8/12 and 5/10 were

320 positive for nares, respectively (Figure 3a). These rates of false negatives are similar, as compared to the
321 37.5% false negative rate reported for plastic-shafted polyester-tipped nasal swabs collected in VTM and
322 extracted from the eluent (Wang et al. 2020). As the degree of viral shedding is known to vary over the
323 course of the disease [23], we compared the performance in the subset of COVID-19(+) patients with an
324 NP-positive swab result within 72 hours of the time of sampling, and observed reduced false negative rates
325 of 18.2% (PE), 25% (TMI), and 30% (CGp). We next compared success rates across swab samples from
326 the built environment. On the floor samples, the CGp had the highest success rate at 75% in detection of
327 SARSs-CoV-2 from SARSs-CoV-2 positive patient rooms whereas PE detected SARSs-CoV-2 in 63% of
328 rooms, and TMI in 44% of rooms (Figure 3a). Bedrail samples had the lowest frequency of detection, 5/16
329 (31%), for each swab type (Figure 3a). For SARSs-CoV-2 negative patients admitted to the same hospital
330 for other reasons, all nares and bedrail samples were negative, whereas one floor sample using the PE swab
331 detected SARSs-CoV-2 (Figure 3b).
332
333 The observed differences in detection among nares and environmental samples, taken in context of results
334 that Since our previous experiment demonstrates that suggest swab type does not impact SARSs-CoV-2
335 detection, this suggests that variation in sample collection from the nares and other environmental samples
336 has an important role in detection sensitivity. When swabbing an environmental surface or body site (i.e.,
337 nares), there is inherent variation in the swabbing event which can be attributed both to stochastic
338 differences in biomass (human cells, dust, etc.) and the overall assay (nucleic acid extraction and RT-
339 qPCR). To evaluate if certain sampling locations or swab types were more variable than others, we
340 calculated the intra-assay coefficient of variance (CV) of the Cq values. The CV was significantly higher
341 in patient nasal samples compared to control (RNA spike-in) samples (P=0.0018), with a median difference
342 in variance of 2.5 (Supplemental S6a). Swab types also demonstrated an effect with CGp and PE differences
343 being significant as compared to the control (P=0.0012) (Supplemental Figures S6b).
344
345 *Microbiome analysis*

346 To determine the feasibility of co-opting nucleic acid for microbiome processing, we processed a subset of
347 samples (n=40) spanning a total of three patients, two sample types (floor and nasal) and the three swab
348 types. After processing with Deblur, the total number of reads per sample were compared (Figure 4a). Read
349 counts were highly variable across sample types and for each patient but were consistent within the swab
350 types for each comparison. For floor samples in patient room 18, PE swabs had the highest number of reads
351 followed by TMI and CGp. For nasal samples however, patient 1 had the higher read counts from TMI
352 while patient 7 and 18 both showed slightly lower read counts for PE swabs as compared to alternative
353 swabs. The differences were minor however and are primarily differentiated by patient room (Figure 4a).
354 After rarifying to 5000 reads a PCoA plot was generated from using Unweighted UniFrac distances (Figure
355 4b). Samples which were collected using different swab types clustered together when controlling for
356 patient room and sample type, suggesting indicating that the swab type used does not have a negative impact
357 on microbiome analysis (Figure 4b). When analyzing all samples together, sample_type (floor vs nasal)
358 and patient number (7 vs 18) were both significant drivers of the microbiome community (sample_type:
359 PERMANOVA n=24, group=2, P=0.001, Fstat=6.94; patient_num PERMANOVA n=24, group=2,
360 P=0.001, Fstat=6.92) whereas swab type did not have an effect (P=0.164). Distances between swab types
361 were lower than distances between patients for both floor (Supplemental Figure S7a) and nasal
362 (Supplemental Figure S7b) samples, with patient 7 exhibiting higher variation than patient 18. Floor
363 samples generally had a higher microbial diversity compared to nasal swabs, with *Staphylococcus*,
364 *Corynebacterium*, *Pseudomonas*, *Streptococcus*, and Enterobacteriaceae being the more dominant taxa.
365 Nasal samples however were mostly enriched by either *Staphylococcus* or *Corynebacterium*, with patient
366 7 having a higher abundance of *Lawsonella* (Figure 4c).
367
368 **Discussion**
369 When assessing whether it will be possible to adapts and switch collection methodology to enable more
370 affordable, more widely available, and more inter-assay compatible collection methods for SARS-CoV-2
371 monitoring, it is key to understand the feasibility of using both alternative swabs and sample storage

372 solutions. Here we provide evidence that the variation observed in a given SARSs-CoV-2 experiment is
373 primarily driven by the time and method of sample collection rather than by the swab type, storage solution,
374 and subsequent extraction and RT-qPCR. When using alcohol-based storage solutions, we demonstrate that
375 the nucleic acid or viral particles tend to become enriched on the swab head rather than the eluent and thus
376 we recommend extracting directly from the swab head itself. We demonstrate that RNA can be successfully
377 extracted from consumer-grade swabs stored in alcohol without compromising RNA integrity or yield. Of
378 note, wooden-shafted swabs performed poorly only when extracting from the eluent, suggesting that RNA
379 adsorption onto the shaft, rather than RT-qPCR inhibitors, may be the source of interference with current
380 eluent-based testing methods for this swab type. As cotton-tipped swabs and alcohol-based storage
381 solutions are compatible with standard microbiome- and metabolome analyses not feasible with VTM, these
382 alternatives could enable more widespread assessment of the microbial context of SARS-CoV-2 RNA in
383 human and environmental samples, including associated microbiome features.
384
385 We also provide preliminary evidence that nasal samples collected using more widely available, consumer-
386 grade, cotton-tipped swabs can be used to detect SARS-CoV-2 in the clinical setting. As cotton-tipped TMI
387 swabs had only a marginally reduced performance compared to CDC-compliant PE swabs for nasal samples
388 compared to NP results, these swabs provide the potential as an attractive alternative for methods such as
389 metabolomics that are complicated by the background from incompatible with polyester-tipped swabs, as
390 well as suggesting the expanding the pool of available medical-grade collection consumables could be
391 expanded. Notably, this variation is less than that observed when comparing different methods for assessing
392 the presence of SARS-CoV-2. Larger-scale testing will be needed to expand and confirm these findings,
393 but our data suggests that these two swab types, in either 95% EtOH or isopropanol, would provide a
394 valuable starting point.
395
396 When considering environmental sampling, our data suggest that TMI and CGp swabs may outperform or
397 at least are similar to, CDC-compliant PE swabs for collecting samples to detect SARS-CoV-2 from floor
398 samples. We provide molecular evidence demonstrating the feasibility of detecting SARs-CoV-2 from floor

samples with a limit of detection (*ca.* 362.5 copies per extraction for TMI) and (750-1450 copies per extraction for CGp and PE) similar to that of other published studies (500 copies per extraction) [24]. Additional testing using pre-wetted swab heads, as performed in other built-environment studies [25–29], is warranted to determine if this would improve the ability of all swab types to detect SARS-CoV-2 in the hospital room environment. The detection of SARS-CoV-2 on *ca.* 50% of COVID-19(+) participants' bedrails and *ca.* 75% of floors, as well as the detection of SARS-CoV-2 on the floor of one non-COVID patient, suggests increased cleaning measures may need to be taken. Indeed, the floor may be a potentially important reservoir for viral exposure, as shoe-covers are not currently recommended by the CDC. However, additional testing is needed to determine whether viable virus particles remain on these surfaces. Since detection largely does not differ across swab types, this suggests that differences seen in the quantitation of SARSs-CoV-2 in the clinic in a given floor or nasal sample is due to variation in the swabbing event itself rather than a molecular processing problem. Because of this, we recommend the need for standardization in medical devices used to collect both nasal and environmental samples specific to SARSs-CoV-2 to improve overall accuracy. Lastly, our efforts to quantify the total noise in a given sampling event and sample processing itself demonstrate how variation in the act of swabbing combined with sample processing may lead to variance and at times lower than expected specificity.

Secondary infections are an important and significant contributing factor to morbidity and mortality in COVID-19 patients [30,31]. With metagenomics assays becoming more common for infectious disease diagnostics in the clinic [32–34], developing molecular methods which enable simultaneous viral detection and metagenomic analysis is critical for understanding disease progression in at-risk populations. Since the storage method is a critical step in preserving microbiome integrity with 95% ethanol as a stable solution [35], our results further demonstrate and open the door for multi-omics processing and analysis of SARSs-CoV-2 samples.

In summary, our results suggest detection of SARS-CoV-2 RNA in the environment could be performed using less expensive, consumer-grade materials and alcohol-based storage solutions. With the materials

examined in this study, it is further conceivable that patients could collect samples from themselves, their environments at home, or their place of work, dramatically expanding the ability to deploy widespread methods for monitoring and predicting outbreak events. Additional confirmatory studies using consumer-grade swabs would greatly support COVID-19 screening worldwide, particularly in resource-limited communities.

Acknowledgements:

We thank research participants who donated samples, the health care professionals who assisted in the collection of samples, and Alison Vrbanac, Louis-Felix Nothias-Scaglia, and Shi Huang for assistance in transportation and Dominic Nguyen for sampling kit preparation. This research benefited tremendously from lessons learned and techniques developed in the Sloan Microbiology of the Built Environment (MoBE program). We thank Stanley T. Motley for early discussion on nucleic acid stability, Sandrine Miller-Montgomery for guidance in RT-qPCR analyses. We thank Thomas F. Rogers and Nathan Beutler for providing the SARS-CoV-2 viral RNA used as a control in this study and David Pride for supplying samples from NP swabs in VTM for our comparisons.

This work was supported by the UC San Diego Center for Microbiome Innovation (CMI). JJM is supported by the National Science Foundation Center for Aerosol Impacts on Chemistry of the Environment #1801971. CM is supported by NIDCR NRSA F31 Fellowship 1F31DE028478-01. PBF is partially funded through trainee support from Sanitarium Health and Wellbeing in partnership with the CMI. DM is partially funded by support from Danone Nutricia Research in partnership with the CMI. JPS is supported by NIH-SD-IRACDA (5K12GM068524-17) and USDA-NIFA (2019-67013-29137).

References:

1. Mediterranean 828 Deaths Eastern, Cases 98, Europe 664 Deaths, Cases 2. 827 789, Pacific 224 Deaths Western, Cases 31 749, et al. Situation in numbers (by WHO Region). Available from: https://www.who.int/docs/default-source/coronaviruse/situation-reports/20200708-covid-19-sitrep-170.pdf?sfvrsn=bca86036_2

2. Gilbert JA, Stephens B. Microbiology of the built environment. Nat Rev Microbiol. 2018;16:661–70.

3. CDC Background F. Environmental Sampling [Internet]. 2019 [cited 2020 Jul 9]. Available from: https://www.cdc.gov/infectioncontrol/guidelines/environmental/background/sampling.html

4. Centers for Disease Control and Prevention. Centers for Disease Control and Prevention SOP#: DSR-052-02- PREPARATION OF VIRAL TRANSPORT MEDIUM [Internet]. Centers for Disease Control and Prevention- PREPARATION OF VIRAL TRANSPORT MEDIUM. 2020 [cited 2020 Apr 24]. Available from: https://www.cdc.gov/coronavirus/2019-ncov/downloads/Viral-Transport-Medium.pdf

5. Kalantar-Zadeh K, Ward SA, Kalantar-Zadeh K, El-Omar EM. Considering the Effects of Microbiome and Diet on SARS-CoV-2 Infection: Nanotechnology Roles. ACS Nano [Internet]. 2020; Available from: http://dx.doi.org/10.1021/acsnano.0c03402

6. Bergner LM, Orton RJ, da Silva Filipe A, Shaw AE, Becker DJ, Tello C, et al. Using noninvasive metagenomics to characterize viral communities from wildlife. Mol Ecol Resour. 2019;19:128–43.

7. Oropharyngeal 1., Swabs N. Collection of Upper Respiratory Tract Specimens. Available from: https://www.cdc.gov/urdo/downloads/SpecCollectionGuidelines.pdf

8. CDC/DDID/NCIRD/ Division of Viral Diseases. CDC 2019-Novel Coronavirus (2019-nCoV) Real-Time RT-PCR Diagnostic Panel. 2020; Available from: https://www.fda.gov/media/134922/download

9. Marx V. Coronavirus jolts labs to warp speed. Nat Methods. 2020;17:465–8.

10. Minich JJ, Zhu Q, Janssen S, Hendrickson R, Amir A, Vetter R, et al. KatharoSeq Enables High-Throughput Microbiome Analysis from Low-Biomass Samples. mSystems [Internet]. 2018;3. Available from: http://dx.doi.org/10.1128/mSystems.00218-17

11. CDC. Coronavirus Disease 2019 (COVID-19) [Internet]. Centers for Disease Control and Prevention. 2020 [cited 2020 Apr 21]. Available from: https://www.cdc.gov/coronavirus/2019-ncov/lab/rt-pcr-panel-primer-probes.html

12. Minich JJ, Humphrey G, Benitez RAS, Sanders J, Swafford A, Allen EE, et al. High-Throughput Miniaturized 16S rRNA Amplicon Library Preparation Reduces Costs while Preserving Microbiome Integrity. mSystems [Internet]. 2018;3. Available from: http://dx.doi.org/10.1128/mSystems.00166-18

13. Apprill A, McNally S, Parsons R, Weber L. Minor revision to V4 region SSU rRNA 806R gene primer greatly increases detection of SAR11 bacterioplankton [Internet]. Aquatic Microbial Ecology. 2015. p. 129–37. Available from: http://dx.doi.org/10.3354/ame01753

14. Caporaso JG, Lauber CL, Walters WA, Berg-Lyons D, Lozupone CA, Turnbaugh PJ, et al. Global patterns of 16S rRNA diversity at a depth of millions of sequences per sample [Internet]. Proceedings of the National Academy of Sciences. 2011. p. 4516–22. Available from: http://dx.doi.org/10.1073/pnas.1000080107

15. Walters W, Hyde ER, Berg-Lyons D, Ackermann G, Humphrey G, Parada A, et al. Improved Bacterial 16S rRNA Gene (V4 and V4-5) and Fungal Internal Transcribed Spacer Marker Gene Primers for Microbial Community Surveys. mSystems [Internet]. 2016;1. Available from: http://dx.doi.org/10.1128/mSystems.00009-15

16. Parada AE, Needham DM, Fuhrman JA. Every base matters: assessing small subunit rRNA primers for marine microbiomes with mock communities, time series and global field samples. Environ Microbiol. 2016;18:1403–14.

493 17. Gonzalez A, Navas-Molina JA, Kosciolek T, McDonald D, Vázquez-Baeza Y, Ackermann G, et al.
494 Qiita: rapid, web-enabled microbiome meta-analysis. Nat Methods. 2018;15:796–8.

495 18. Estaki M, Jiang L, Bokulich NA, McDonald D, González A, Kosciolek T, et al. QIIME 2 Enables
496 Comprehensive End-to-End Analysis of Diverse Microbiome Data and Comparative Studies with
497 Publicly Available Data. Curr Protoc Bioinformatics. 2020;70:e100.

498 19. Bolyen E, Rideout JR, Dillon MR, Bokulich NA, Abnet CC, Al-Ghalith GA, et al. Reproducible,
499 interactive, scalable and extensible microbiome data science using QIIME 2. Nat Biotechnol.
500 2019;37:852–7.

501 20. Amir A, McDonald D, Navas-Molina JA, Kopylova E, Morton JT, Zech Xu Z, et al. Deblur Rapidly
502 Resolves Single-Nucleotide Community Sequence Patterns. mSystems [Internet]. 2017;2. Available from:
503 http://dx.doi.org/10.1128/mSystems.00191-16

504 21. Vázquez-Baeza Y, Pirrung M, Gonzalez A, Knight R. EMPeror: a tool for visualizing high-
505 throughput microbial community data. Gigascience. 2013;2:16.

506 22. Schroeder A, Mueller O, Stocker S, Salowsky R, Leiber M, Gassmann M, et al. The RIN: an RNA
507 integrity number for assigning integrity values to RNA measurements. BMC Mol Biol. 2006;7:3.

508 23. Zou L, Ruan F, Huang M, Liang L, Huang H, Hong Z, et al. SARS-CoV-2 Viral Load in Upper
509 Respiratory Specimens of Infected Patients. N Engl J Med. 2020;382:1177–9.

510 24. Vogels CBF, Brito AF, Wyllie AL, Fauver JR, Ott IM, Kalinich CC, et al. Analytical sensitivity and
511 efficiency comparisons of SARS-CoV-2 RT-qPCR primer-probe sets. Nat Microbiol [Internet]. 2020;
512 Available from: http://dx.doi.org/10.1038/s41564-020-0761-6

513 25. Lax S, Cardona C, Zhao D, Winton VJ, Goodney G, Gao P, et al. Microbial and metabolic succession
514 on common building materials under high humidity conditions. Nat Commun. 2019;10:1767.

515 26. Richardson M, Gottel N, Gilbert JA, Lax S. Microbial Similarity between Students in a Common
516 Dormitory Environment Reveals the Forensic Potential of Individual Microbial Signatures. MBio
517 [Internet]. 2019;10. Available from: http://dx.doi.org/10.1128/mBio.01054-19

518 27. Lax S, Sangwan N, Smith D, Larsen P, Handley KM, Richardson M, et al. Bacterial colonization and
519 succession in a newly opened hospital. Sci Transl Med. 2017;9.

520 28. Wood M, Gibbons SM, Lax S, Eshoo-Anton TW, Owens SM, Kennedy S, et al. Athletic equipment
521 microbiota are shaped by interactions with human skin. Microbiome. 2015;3:25.

522 29. Lax S, Smith DP, Hampton-Marcell J, Owens SM, Handley KM, Scott NM, et al. Longitudinal
523 analysis of microbial interaction between humans and the indoor environment. Science. 2014;345:1048–
524 52.

525 30. Alhazzani W, Møller MH, Arabi YM, Loeb M, Gong MN, Fan E, et al. Surviving Sepsis Campaign:
526 Guidelines on the Management of Critically Ill Adults with Coronavirus Disease 2019 (COVID-19). Crit
527 Care Med. 2020;48:e440–69.

528 31. Ruan Q, Yang K, Wang W, Jiang L, Song J. Clinical predictors of mortality due to COVID-19 based
529 on an analysis of data of 150 patients from Wuhan, China. Intensive Care Med. 2020;46:846–8.

530 32. Deng X, Achari A, Federman S, Yu G, Somasekar S, Bártolo I, et al. Metagenomic sequencing with
531 spiked primer enrichment for viral diagnostics and genomic surveillance. Nat Microbiol. 2020;5:443–54.

532 33. Wilson MR, Sample HA, Zorn KC, Arevalo S, Yu G, Neuhaus J, et al. Clinical Metagenomic
533 Sequencing for Diagnosis of Meningitis and Encephalitis. N Engl J Med. 2019;380:2327–40.

534 34. Chiu CY, Miller SA. Clinical metagenomics. Nat Rev Genet. 2019;20:341–55.

535 35. Song SJ, Amir A, Metcalf JL, Amato KR, Xu ZZ, Humphrey G, et al. Preservation Methods Differ in
536 Fecal Microbiome Stability, Affecting Suitability for Field Studies. mSystems [Internet]. 2016;1.
537 Available from: http://dx.doi.org/10.1128/mSystems.00021-16

538

539

540

541

542

543

544

545

546
547

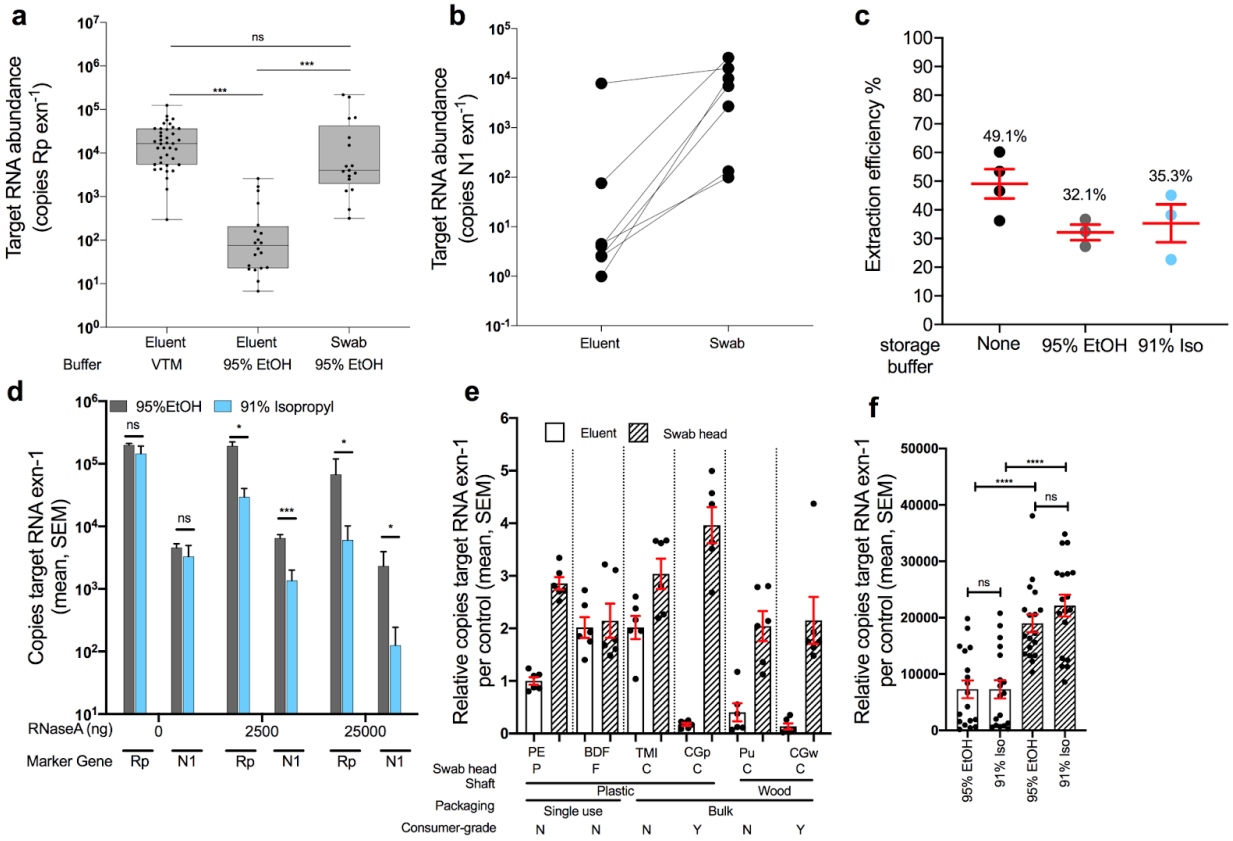

Figure 1. Validation of alternative swabs and storage buffer (95% EtOH and 91% isopropanol) in RNA recovery and detection of COVID-19.

a) Human RNAse P gene (Rp) amplification was used to compare nucleic acid extraction efficiency across sample processing methods. Clinical gold-standard polyester-tipped plastic-shaft NP swabs stored in VTM and extracted from 200 µL of eluent (left, n=39) have significantly higher copy numbers compared to 200 µL EtOH eluent from PE nares swabs (middle, n=22), but not when extracted from the EtOH-preserved swab head (right, n=18). One-way ANOVA with Tukey's multiple comparison VTM eluent vs EtOH eluent p=<0.001, EtOH eluent vs EtOH swab p<0.001, VTM vs EtOH swab p = 0.266. **b)** Extrapolated viral RNA copy number from COVID-19 positive nares samples collected with BD polyester swabs in the hospital stored in 95% EtOH and extracted from either the eluent or swab from the same sample (n=24, one-tailed paired Student's T-test p=0.032). **c)** Proportion of RNA recovered across three storage buffers: None, 95% EtOH, and 91% isopropanol using commercial human RNA added to storage buffers (ns, one-way ANOVA

561 p>0.05). **d)** Evaluation of RNaseA inhibition by 95% EtOH (grey) and 91% isopropanol (blue) using either
562 the human Rp or SARS-CoV-2 N1 primer set on control RNA added to each solution (unpaired t-tests of
563 95% EtOH vs 91% Iso per each marker at 0, 2500, 25000 ng RNaseA). **e)** Comparison human RNA
564 recovery across six swab types (PE=polyester 'commercial', BDF=BD foam 'commercial', TMI=BD TMI
565 'commercial', CGp=plastic 'consumer-grade', Pu=Puritan 'commercial', CGw=wood 'consumer-grade'),
566 extracted from 200µL eluent (blank bar) or the swab head. Recovery for each swab type is normalized to
567 the CDC recommended method (eluent from PE swab). A '2' would indicate there was 2x more RNA
568 recovered whereas a 0.5 would indicate a 50% reduction in RNA recovery. **f)** Total RNA copies per
569 extraction for all samples which are grouped by sample-type (eluent or swab head) and storage buffer (95%
570 EtOH or 91% isopropanol). Pairwise comparisons performed within sample-type (not significant) and
571 across sample-type controlling for storage buffer (Mann-Whitney, U=test statistic).
572
573
574
575
576
577
578
579

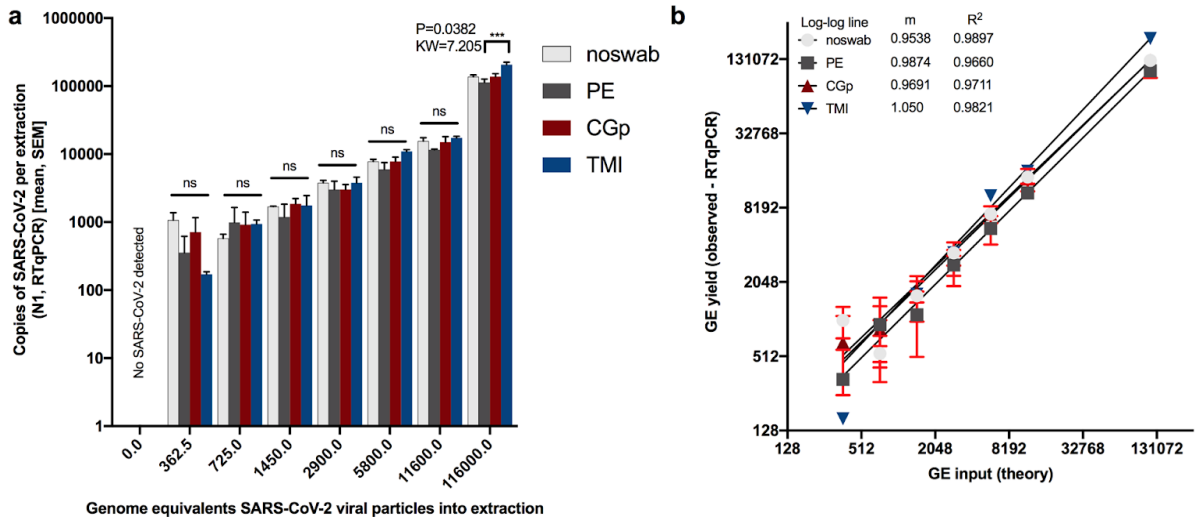

Figure 2. Limit of detection of SARs-CoV-2 viral particles across swab types (Polyester 'PE', CGp, and TMI). "Noswab" refers to direct extraction of viral particles. a) Comparisons of total RNA recovery per extraction across swab types including 'noswab' performed at each dilution (Kruskal Wallis test). Comparison of (theory input Genome Equivalents 'GE') to measured GE of triplicates (mean, SEM) by RTqPCR of SARs-CoV-2. Non-linear regression analysis of each dilution series for noswab, PE, CGp, and TMI swabs.

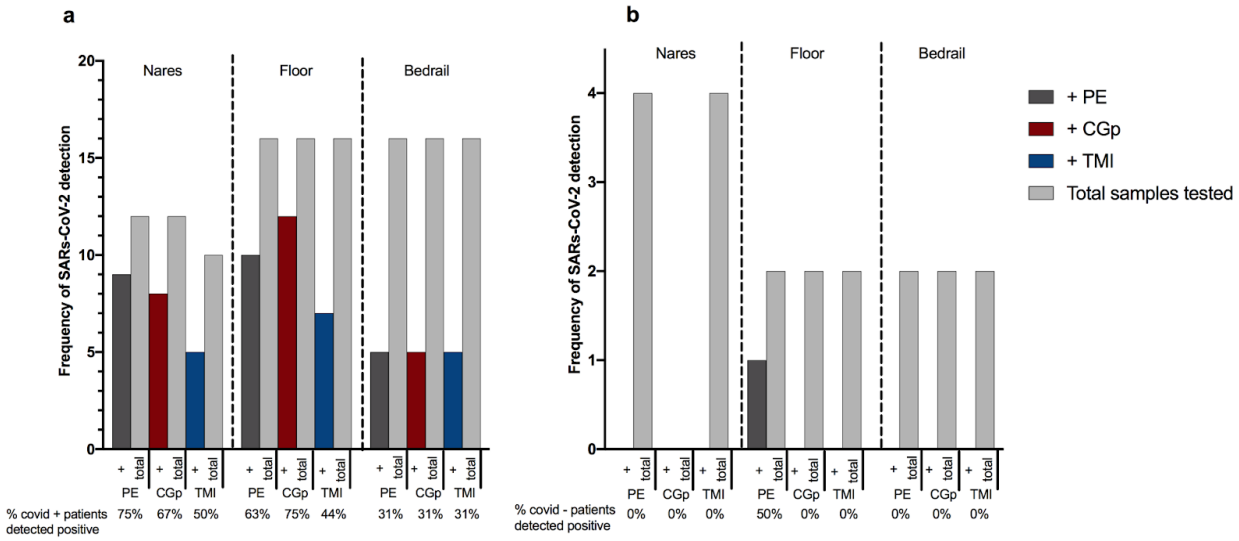

Figure 3: Comparison of CDC approved PE swabs, consumer-grade CGp and bulk TMI swab congruence compared to clinical-grade hospital tests using polyester-tipped plastic shafted NP swabs for twenty participants in the clinical setting. a) SARs-CoV-2 positive patients (n=16) sampled with three swab types across three environments: nares, floor, and bedrail. '+' samples (dark grey = PE, red = CGp, blue = TMI) refer to samples which tested positive for SARs-CoV-2 out of the total samples tested for that particular swab type (light grey bar). Percentage of positive tests per swab type are below x axis for each environmental sample. b) SARs-CoV-2 negative patients (n=4) with three swab types across three environments: nares, floor, and bedrail. Same nomenclature as above.

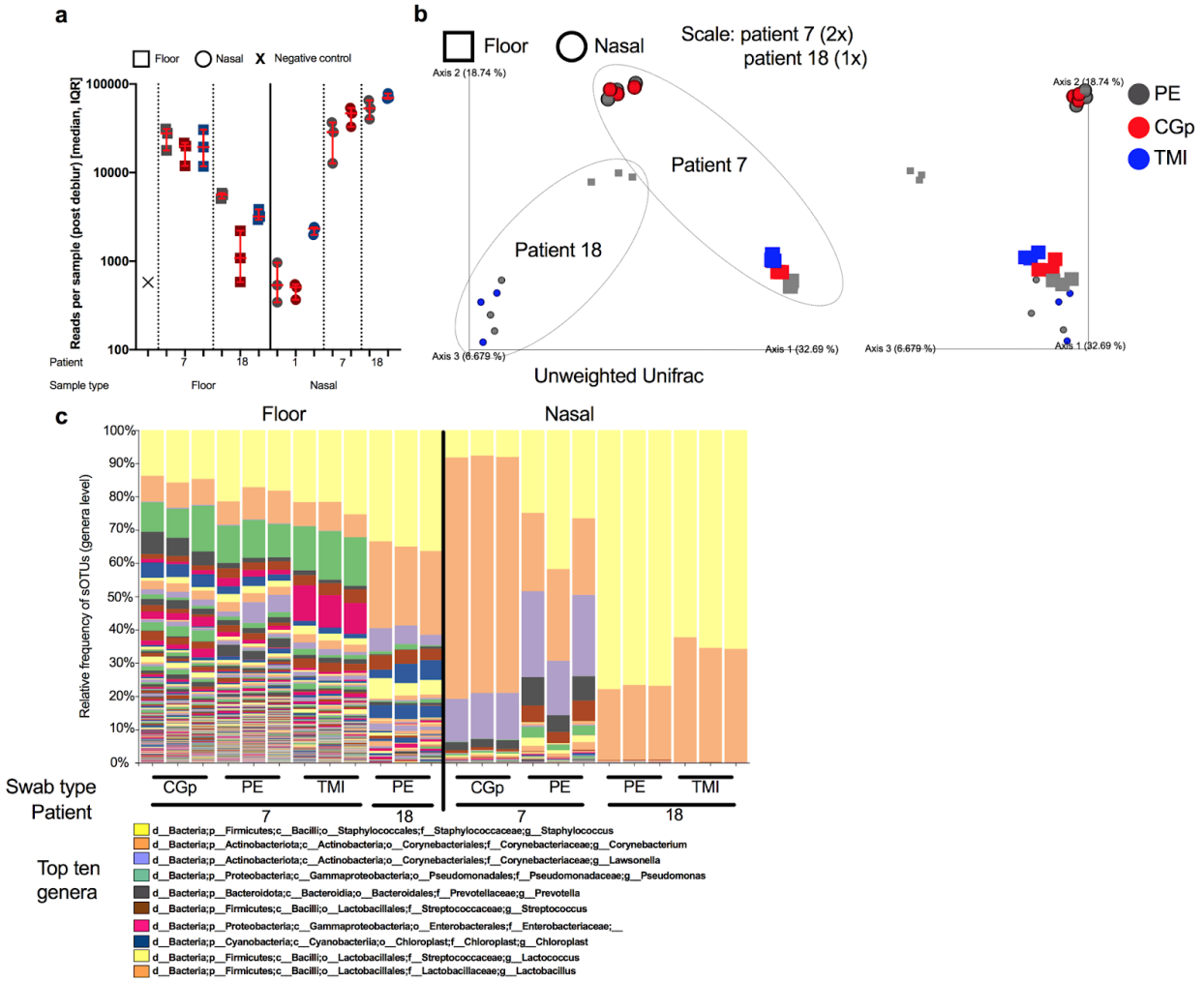

Figure 4. Microbiome 16S rRNA sequencing validation across sample types, patients, and swab types. a) Total number of reads per sample (40 samples sequenced) after processing through deblur pipeline stratified by sample type (floor 'square' vs nasal 'circle'), patient number (1, 7, and 18) and colored by swab type (PE = grey, CGp = red, TMI = blue). Error bars represent median, IQR for triplicate biological replicates per sample. b) Unweighted UniFrac PCoA plot of samples rarified to 5000 reads. Enlarged samples (2x) indicate patient 7 whereas (1x) indicates patient 18. Swab types are colored (PE = grey, CGp = red, TMI = blue) and shapes (floor 'square' vs nasal 'circle') indicate sample type. Grey dotted line goes around each patient. c) Stacked bar plot collapsed at genera level with top ten abundant genera labeled in the legend.

617 **Supplementary Figures and Legends**

618 **Supplemental Table 1.**

Supplemental Table. SARs-CoV-2 Limit of detection: total quantified copies of SARs-CoV-2 (N1 or N2) and human Rp across swab types.												
	N1											
	noswab			PE			CGp			TMI		
0	0	0	0	0	0	0	0	0	0	0	0	0
362.5	1683	749	782	866	0	203	0	600	1539	195	146	173
725	420	599	713	0	2213	752	1585	1175	0	1204	859	755
1450	1704	1722	1665	209	946	2411	1390	1618	2572	1021	3147	1071
2900	4305	3868	3157	1432	2801	4794	4053	2834	2153	2166	4646	4533
5800	7598	6897	8862	3819	8958	5086	5836	10027	7527	12332	10290	10227
11600	19177	14181	13316	11752	11062	11885	20925	10598	13416	17761	18618	15658
116000	138318	121286	151498	104301	139976	94119	163019	111423	138201	212959	233003	172233
	N2											
	noswab			PE			CGp			TMI		
0	0	0	0	0	0	0	0	0	0	0	0	0
362.5	218	0	133	419	0	125	0	0	643	420	131	289
725	719	474	345	308	458	127	217	222	0	356	484	489
1450	263	1356	371	170	345	1099	1550	633	889	1023	1626	61
2900	1536	2525	781	622	1004	1228	1694	1289	937	1587	1146	1371
5800	2350	2764	3261	2718	3527	1733	2924	6110	2246	4861	5149	3254
11600	5230	5572	6646	5569	4899	5883	6011	3656	4922	8808	8611	7388
116000	49810	53165	57606	43923	66597	43910	46084	41405	50328	93101	102074	61855
	Rp											
	noswab			PE			CGp			TMI		
0	0	0	0	521	462	391	347	86	66	0	79	0
362.5	0	0	0	1861	737	283	164	263	185	130	83	0
725	0	0	0	723	3368	921	67	81	0	207	0	0
1450	0	0	0	283	426	499	0	0	377	135	198	147
2900	0	0	0	1254	479	222	194	97	422	0	156	0
5800	0	0	0	252	873	491	0	220	0	97	0	0
11600	0	0	0	149	526	1112	203	426	220	52	77	143
116000	0	0	0	330	798	1047	3980	0	256	117	97	0

619

620
621
622

623

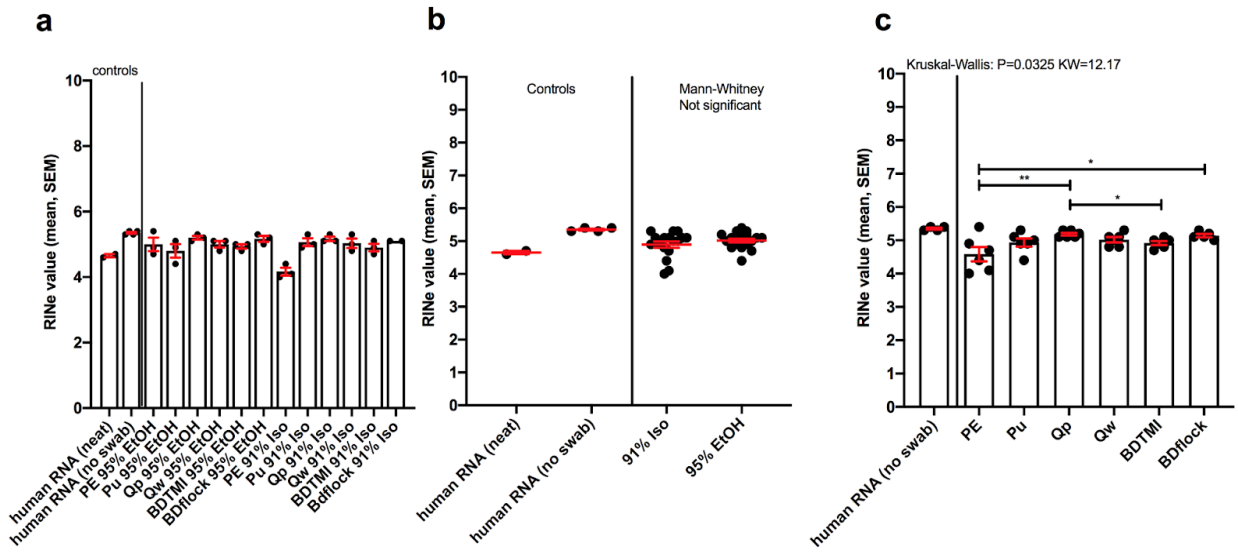

Supplemental Figure 1. Impacts of storage solution or swab type on RNA quality as measured by RNA Tapestation High Sensitivity kit.

a) All direct-swab extracted RNA grouped by storage buffer and swab type. b) Samples grouped by storage buffer, no significant difference in RNA integrity number (RIN) values between storage buffers (95% EtOH vs. 91% isopropanol) (Mann-Whitney). c) Swab extracts grouped by swab type only and compared to determine if swab type has an impact on RNA quality (Kruskal-Wallis test).

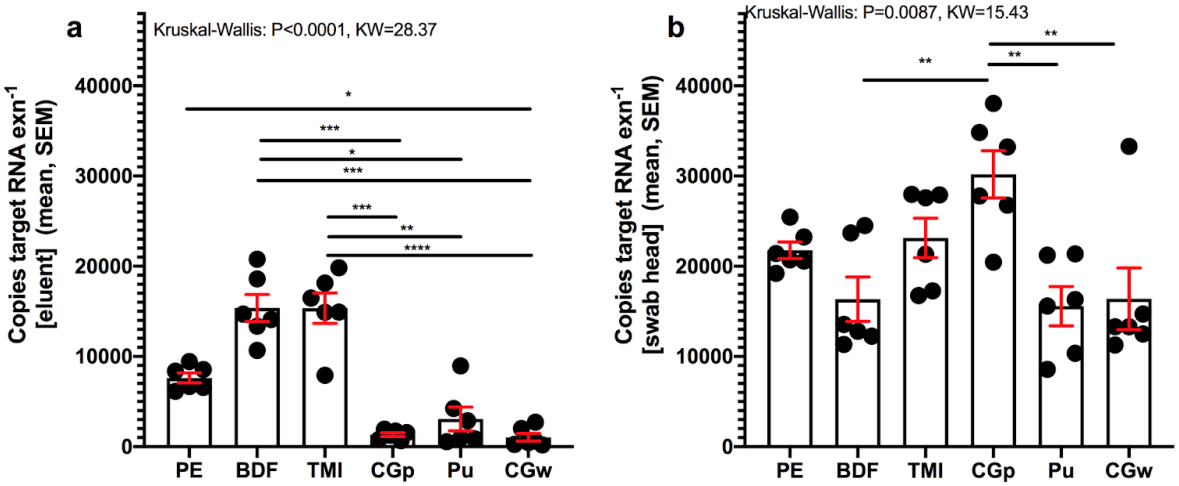

Supplemental Figure 2. Impacts of sample-type (eluent vs. swab head) on RNA recovery by swab used.

Comparison human RNA recovery across six swab types (PE=polyester 'commercial', BDF=BD foam 'commercial', TMI=BD TMI 'commercial', CGp=plastic 'consumer-grade', Pu=Puritan 'commercial', CGw=wood 'consumer-grade'), **a)** extracted from 200 µL eluent or **b)** swab head (Group comparison using Kruskal-Wallis)

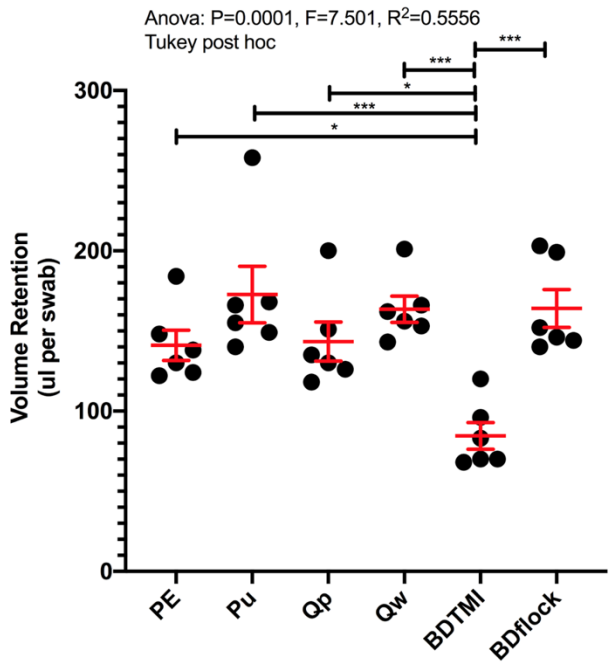

Supplemental Figure 3. Adsorption volumes per swab type.

Samples tested for normality using Shapiro- Wilke test (not significant, P=0.12, W=0.8357).

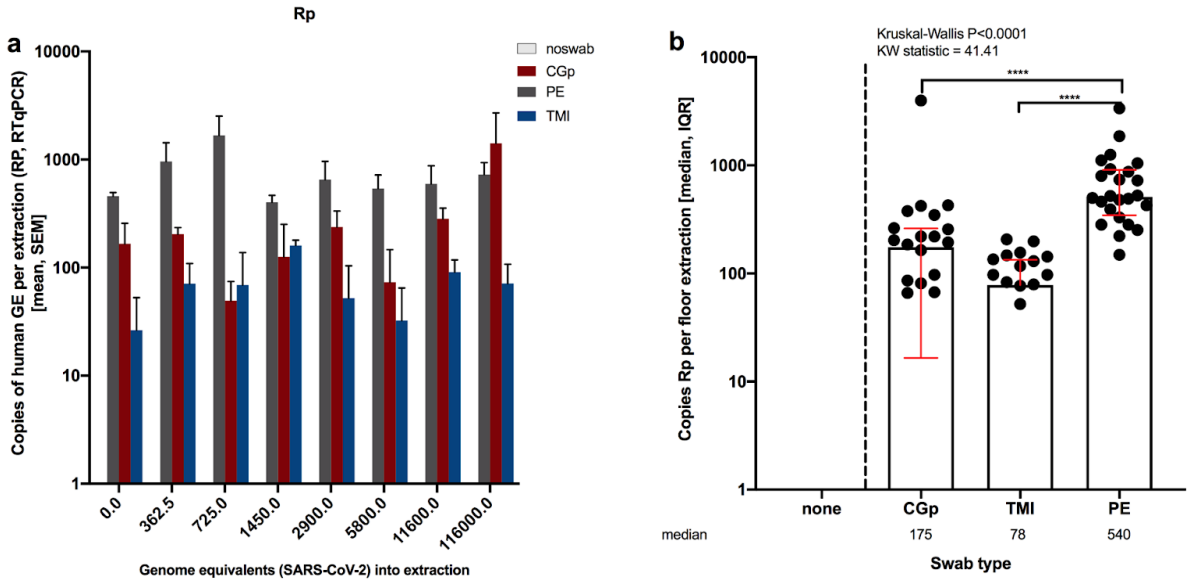

Supplemental Figure 4. Total variation of human Rp gene detected from floor samples in limit of detection experiment. a) Variation of Rp across swab types and subsequent dilutions. b) total yield of human Rp across aggregated swab types.

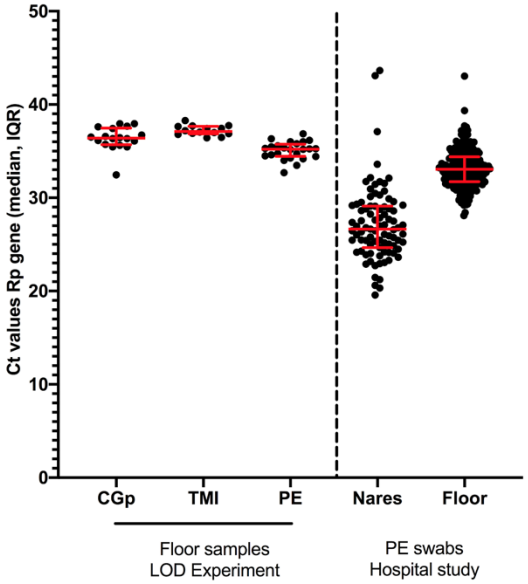

667

668 **Supplemental Figure 5. Variation of human Rp gene amplification across swab types.**

669 (left) Surface swabs were collected from the floor of a laboratory to compare efficiency across swab types;

670 consumer-grade cotton (CGp), The Microsetta Initiative cotton swabs (TMI), and polyester (PE). (right)

671 PE surface swab samples were collected with the same protocol in the hospital. The variation across hospital

672 samples is greater than the variation among swab types.

673
674
675

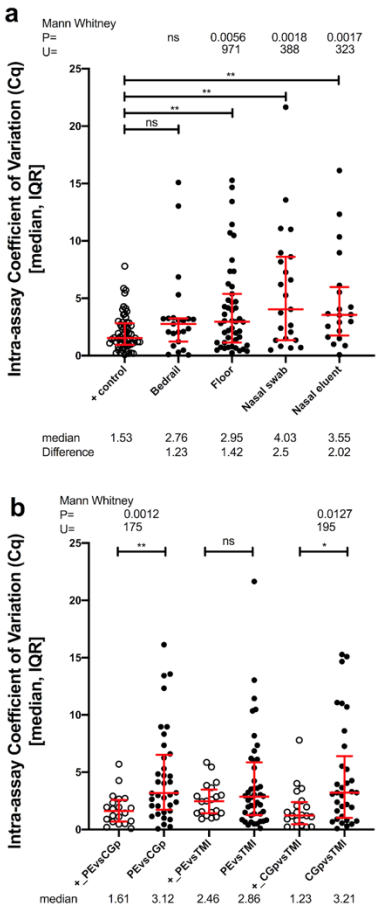

Supplemental Figure 6. Intra-assay variability compared across positive controls, sample _types, and swab types.

a) Coefficient of variance calculated across pairwise swabs taken within each room/patient replicate and then distributions compared for bedrail, floor, nasal swab, and nasal eluent samples along with positive controls. b) The CV was also grouped and compared by swab type.

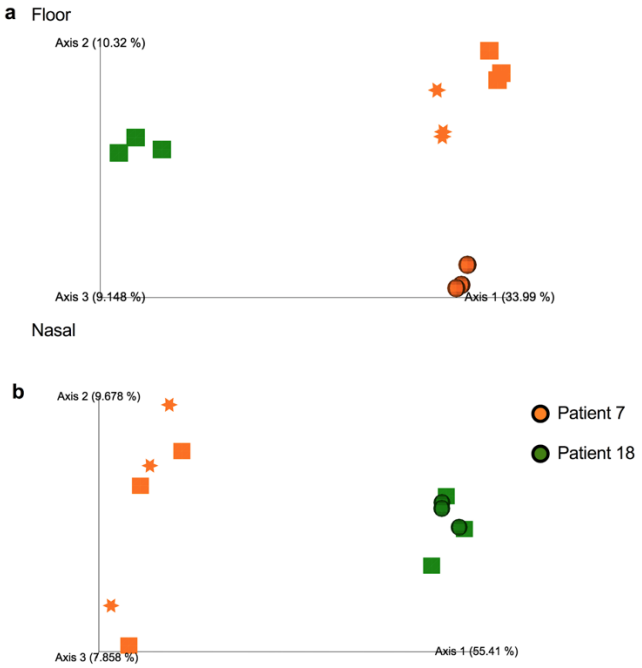

683

684

685 **Supplemental Figure 7.** Comparison of 16S rRNA microbial composition of paired patient and sample

686 type samples collected using different swabs (in triplicate) using Unweighted UniFrac PCoA plot. a) floor

687 samples, b) nasal samples. Swab types: square = PE, circle = CGp, star = TMI.

688

689